Title

The Dialuminene AriPr8AlAlAriPr8 (AriPr8=C6H-2,6-(C6H2-2,4,6-iPr3)2-3,5-iPr2).

Journal

Angewandte Chemie, 63(52)

Authors

Lehmann, Annika

Queen, Joshua

Roberts, Christopher

et al.

Publication Date

2024-12-20

DOI

10.1002/anie.202412599

Peer reviewed

How to cite: *Angew. Chem. Int. Ed.* **2024**, *63*, e202412599
doi.org/10.1002/anie.202412599

Multiple Bonds

The Dialuminene $Ar^{iPr8}AlAlAr^{iPr8}$ ($Ar^{iPr8} = C_6H$-2,6-(C_6H_2-2,4,6-$^iPr_3$)$_2$-3,5-$^iPr_2$)

Annika Lehmann[+], Joshua D. Queen[+], Christopher J. Roberts, Kari Rissanen, Heikki M. Tuononen, and Philip P. Power**

Abstract: Careful analysis of the crystals formed in the reduction of $Ar^{iPr8}AlI_2$ ($Ar^{iPr8} = C_6H$-2,6-(C_6H_2-2,4,6-$^iPr_3$)$_2$-3,5-$^iPr_2$) with sodium on sodium chloride showed them to contain the long sought-after dialuminene $Ar^{iPr8}AlAlAr^{iPr8}$ (**1**) that forms alongside the previously characterized alanediyl :$AlAr^{iPr8}$. The single crystal X-ray structure of **1** revealed a nearly planar, *trans*-bent C(ipso)AlAlC(ipso) core with an Al–Al distance of 2.648(2) Å. The molecular and electronic structure of **1** are consistent with an Al–Al double dative interaction augmented with diradical character and stabilized by dispersion interactions. Density functional theory calculations showed that the reactivity of :$AlAr^{iPr8}$ with dihydrogen involves **1**, not :$AlAr^{iPr8}$, as the reactive species. In contrast, the reaction of :$AlAr^{iPr8}$ with ethylene gave two products, the 1,4-dialuminacyclohexane $Ar^{iPr8}Al(C_2H_4)_2AlAr^{iPr8}$ (**2**) and the aluminacyclopentane $Ar^{iPr8}Al(C_4H_8)$ (**3**), that can both form from the aluminacyclopropane intermediate $Ar^{iPr8}Al(C_2H_4)$. Although the [2+2+2] cycloaddition of **1** with two equivalents of ethylene was also calculated to be exergonic, it is likely to be kinetically blocked by the numerous isopropyl substituents surrounding the Al–Al bond. Attempts to fine-tune the steric bulk of the terphenyl ligand to allow stronger Al–Al bonding were unsuccessful, leading to the isolation of the sodium salt of a cyclotrialuminene, $Na_2[AlAr^{iPr6}]_3$ (**4**), instead of $Ar^{iPr6}AlAlAr^{iPr6}$.

Introduction

The report of the salt $Na_2[Ar^{iPr6}GaGaAr^{iPr6}]$ (**Ib**, $Ar^{iPr6} = C_6H_3$-2,6-(C_6H_2-2,4,6-$^iPr_3$)$_2$) by Robinson in 1997 generated great interest since its dianionic moiety $[Ar^{iPr6}GaGaAr^{iPr6}]^{2-}$, which has a planar, *trans*-bent C(ipso)GaGaC(ipso) core and an extremely short Ga–Ga distance (2.319(3) Å), was stated to have a Ga≡Ga triple bond, that is, a digallyne derivative by analogy to alkynes (Figure 1).[1] Later, its related aluminum analog $Na_2[Ar^{iPr4}AlAlAr^{iPr4}]$ (**Ia**, $Ar^{iPr4} = C_6H_3$-2,6-(C_6H_3-2,6-$^iPr_2$)$_2$) was shown to have a similar *trans*-bent structure for its $[Ar^{iPr4}AlAlAr^{iPr4}]^{2-}$ core and a short Al–Al bond (2.428(1) Å).[2] Further investigations showed that the related neutral, formally double bonded group 13 dimetallenes $Ar^{iPr4}MMAr^{iPr4}$ (Figure 1) were obtainable by reaction of $LiAr^{iPr4}$ with the metal monohalides (**IIb–d**, M = Ga, In, or Tl).[3–5] The dimetallenes were found to dissociate to metallanediyls :MAr^{iPr4} in solution, underlining the weak-

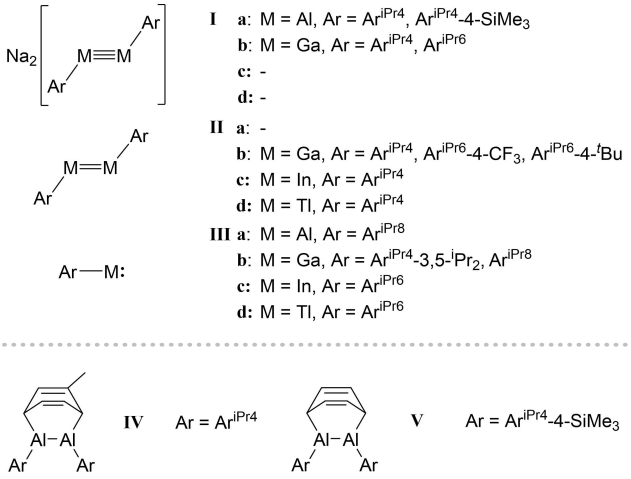

Figure 1. Structurally characterized terphenyl-substituted group 13 dimetallynes (**I**), dimetalleneds (**II**), and metallanediyls (**III**) along with selected examples of cycloaddition products of dialuminenes with arene solvents (**IV** and **V**). $Ar^{iPr4} = C_6H_3$-2,6-(C_6H_3-2,6-$^iPr_2$)$_2$, $Ar^{iPr6} = C_6H_3$-2,6-(C_6H_2-2,4,6-$^iPr_3$)$_2$, and $Ar^{iPr8} = C_6H$-2,6-(C_6H_2-2,4,6-$^iPr_3$)$_2$-3,5-$^iPr_2$.

[*] A. Lehmann,[+] C. J. Roberts, Prof. Dr. K. Rissanen, Prof. Dr. H. M. Tuononen
Department of Chemistry
University of Jyväskylä
P.O. Box 35, FI-40100 Jyväskylä, Finland
E-mail: heikki.m.tuononen@jyu.fi
Dr. J. D. Queen,[+] Prof. Dr. P. P. Power
Department of Chemistry
University of California
One Shields Avenue, Davis, California, USA 95616
E-mail: pppower@ucdavis.edu
Dr. J. D. Queen[+]
Present address:
Department of Chemistry, 1120 Natural Sciences II, University of California, Irvine, California, USA, 92697-2025
[+] These authors contributed equally

ness of their M–M bonds. Isolation of the group 13 diyls in the solid state (Figure 1) could be accomplished by using the bulkier Ar^{iPr6} (**IIIc**,**d**, M = In or Tl)[6,7] and Ar^{iPr4}-3,5-$^{i}Pr_2$ or Ar^{iPr8} (**IIIb**, M = Ga, Ar^{iPr4}-3,5-$^{i}Pr_2 = C_6H$-2,6-(C_6H_3-2,6-$^{i}Pr_2)_2$-3,5-$^{i}Pr_2$, $Ar^{iPr8} = C_6H$-2,6-(C_6H_2-2,4,6-$^{i}Pr_3)_2$-3,5-$^{i}Pr_2$)[8] ligands. These findings, in combination with theoretical work,[9–11] indicated that the dimetallynes have two weak donor-acceptor bonds and a π-bond, showing that they are indeed formal analogues of alkynes.

Despite the breadth of results pertaining to terphenyl-stabilized group 13 dimetallynes and dimetallenes, it has proved particularly difficult to isolate and characterize neutral dialuminenes of the type ArAlAlAr (**IIa**). First attempts to isolate a stable example employing the Ar^{iPr4} ligand led to a species in which the target dialuminene had formed a cycloaddition product with a molecule of toluene (**IV**, Figure 1).[12] In a similar vein, while decorating the Ar^{iPr4} ligand with a $SiMe_3$ substituent improved the solubility of the dialuminene in non-aromatic solvents, the compound proved unstable and could only be isolated as a benzene complex (**V**, Figure 1).[13] To reduce the reactivity of the dialuminene and prevent cycloaddition with aromatic solvents, we sought to increase the steric demand of the terphenyl ligand by introducing isopropyl substituents at the *meta*-positions of the central aryl ring, affording the -Ar^{iPr8} ligand. Application of this ligand to aluminum allowed us to generate orange-yellow crystals that were shown to be the monomeric alanediyl :$AlAr^{iPr8}$ (**IIIa**) by X-ray crystallography.[14] However, the reaction mixture from the synthesis of :$AlAr^{iPr8}$ also gave green crystals which proved difficult to characterize. Nevertheless, the collection and analysis of numerous X-ray crystallographic data sets ultimately permitted an accurate structural solution. Herein, we present the results of this work showing that the unknown species is the sought-after dialuminene of the type **IIa**, that is, $Ar^{iPr8}AlAlAr^{iPr8}$ (**1**, Figure 2), that crystallizes alongside :$AlAr^{iPr8}$ from the reductive dehalogenation of $Ar^{iPr8}AlI_2$. We also present experimental and computational evidence that the reactivity of the diyl :$AlAr^{iPr8}$ with dihydrogen proceeds via the dialuminene **1**, whereas its reactivity with ethylene most likely involves only the diyl. The results of the attempted syntheses of $Ar^{iPr6}AlAlAr^{iPr6}$ are also reported.

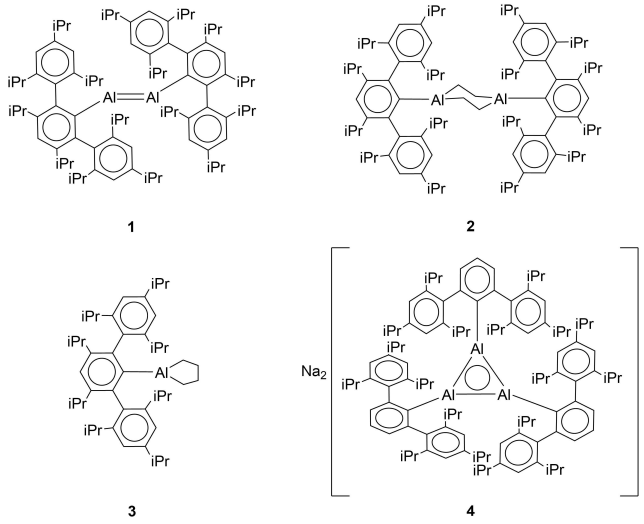

Figure 2. Compounds synthetized and characterized in this work.

Results and Discussion

Synthesis and Characterization of $Ar^{iPr8}AlAlAr^{iPr8}$

We recently reported that the reductive dehalogenation of $Ar^{iPr8}AlI_2$ with an excess of freshly prepared Na on NaCl in hexanes gave dark red solutions from which the monomeric alanediyl :$AlAr^{iPr8}$ could be obtained via recrystallization from C_6D_6 at ca. 8 °C.[14] In addition to orange-yellow crystals of :$AlAr^{iPr8}$, highly sensitive green blocks were formed repeatedly and consistently, but in varying proportion (see SI). Manual separation of the crystals and subsequent structural analysis by single crystal X-ray diffraction showed the green crystals to be the dialuminene $Ar^{iPr8}AlAlAr^{iPr8}$ (**1**). Detailed analysis of the raw diffraction data indicated that the crystal quality had degraded over the course of data collection (see SI), possibly because of the extreme reactivity of the compound, evaporation of the lattice solvent, cryo-cooling of the sample, or a combination of thereof. In addition, the aluminum atoms were found to be surrounded by anomalous maxima in the residual electron density map which, however, diminished significantly when solvent disorder was treated appropriately (highest peak 1.78 e Å^{-3}). Despite several data collections, no improvement in the solution and refinement of the structure was achieved.

The structure of **1** (Figure 3) is a dimer comprised of formally doubly bonded :$AlAr^{iPr8}$ units with a nearly planar, *trans*-bent C(ipso)AlAlC(ipso) core. The Al–Al and Al–C(ipso) distances are 2.648(2) and 1.996(3)/2.013(3) Å, respectively, and the two Al–Al–C(ipso) angles are 129.5(1)° and 133.6(1)°. As is apparent from the structure, the plane of the central aryl ring in one of the terphenyl ligands is almost parallel to the C(ipso)AlAlC(ipso) core (16.3°), whereas the other central ring plane lies almost perpendicularly to it (82.0°). The flanking aryl rings are essentially perpendicular to the central ring to which they are attached. The structural parameters within the Ar^{iPr8} ligands are normal with no major deviations from expected values. A comparison of the structure of **1** to data for related species shows that the Al–Al distance in it is ca. 0.2 Å longer than those in the dialuminynes $Na_2[Ar^{iPr4}AlAlAr^{iPr4}]$ (2.493(2) Å)[2] and $Na_2[(Ar^{iPr4}$-4-$SiMe_3)AlAl(Ar^{iPr4}$-4-$SiMe_3)]$ (2.4255(6) and 2.4268(6) Å),[13] while being comparable to the Al–Al separation in the dialane $Ar^{iPr8}Al(H)(\mu$-$H)_2Al(H)Ar^{iPr8}$ (2.6363(9) Å) with no Al–Al bond.[15]

Redissolving the green crystals of **1** in hexanes gave a green solution whose electronic spectrum (see SI) showed two main absorptions at 354 and 454 nm, indicative of dissociation to :$AlAr^{iPr8}$.[14] Two weak absorptions with a maximum at 650 and a shoulder at ca. 770 nm were also observed, which are presumably responsible of the green

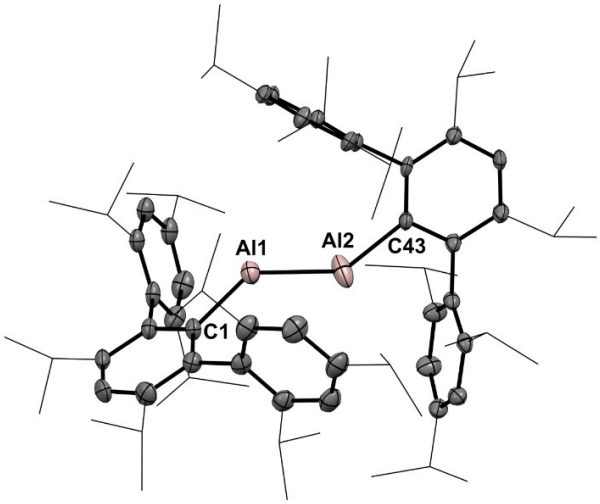

Figure 3. Single crystal X-ray structure of $Ar^{iPr8}AlAlAr^{iPr8}$ (**1**) with carbon atoms of the isopropyl groups shown in wireframe format and hydrogen atoms not shown. Thermal ellipsoids are drawn at 50% probability level. Selected bond lengths (Å) and angles (°) with calculated values in square brackets: Al1–Al2 = 2.648(2) [2.680]; Al1–C1 = 1.996(3) [2.009], Al2–C43 = 2.013(3) [2.015], Al1–Al2–C43 = 133.6(1) [128.3], Al2–Al1–C1 = 129.5(1) [127.2], C1–Al1–Al2–C43 = −173.8(2) [−174.0].

color and are tentatively assigned to **1**. In contrast, redissolving the green crystals of **1** in C_6D_6 resulted in a yellow solution that on the basis of ^{1}H NMR spectroscopy contains a mixture of products (see SI). Besides features characteristic of $:AlAr^{iPr8}$,[14] the ^{1}H NMR data also indicated the presence of Al–H protons, suggestive of the formation of the dialane $Ar^{iPr8}Al(H)(\mu\text{-}H)_2Al(H)Ar^{iPr8}$ in solution,[16] though the experimental data are not entirely consistent with this structural formulation. In the light of this result, the possibility that the crystals of **1** contained $Ar^{iPr8}Al(H)(\mu\text{-}H)_2Al(H)Ar^{iPr8}$ as a contaminant was considered. Although the dialane is used as a starting material in the synthesis of $Ar^{iPr8}AlI_2$, no impurities could be detected in the diiodide by ^{1}H NMR spectroscopy. In addition, the residual electron density maxima in the crystallographic data for **1** do not coincide with the locations of bridging and terminal hydrogen atoms expected in the structure of $Ar^{iPr8}Al(H)(\mu\text{-}H)_2Al(H)Ar^{iPr8}$, though the Al–Al and Al–C(ipso) distances in **1** and $Ar^{iPr8}Al(H)(\mu\text{-}H)_2Al(H)Ar^{iPr8}$ are markedly similar.[15] Furthermore, the gas phase optimized geometry of **1** is an excellent match with the experimental structure (Figure 3), save for the relative orientation of the central aryl rings that is affected by the solvent molecules in the crystal lattice, supporting the crystallographic assignment. At this point, the origin of the ^{1}H NMR signals for the Al–H protons cannot be conclusively explained, but the extreme reactivity of **1** could allow intra- and/or intermolecular C–H activation, presumably leading to the formation of Al–H moieties. This is similar to the reactivity observed by Braunschweig for the transient carbene-supported dialuminene Ar^{Me6}-(^{4Me}NHC)AlAl(^{4Me}NHC)Ar^{Me6} ($Ar^{Me6} = C_6H_3$-2,6-(C_6H_2-2,4,6-Me_3)$_2$, ^{4Me}NHC = 1,3,4,5-tetramethylimidazol-2-ylidene).[17] The compound is isolated as the intramolecular cycloaddition product with a flanking ring of the Ar^{Me6} ligand. Upon heating in benzene, it underwent C–H activation with one of the Ar^{Me6} methyl groups.

The frontier Kohn–Sham orbitals of **1** show the expected features.[11] Specifically, HOMO-1 is a σ-type Al–Al bonding orbital, HOMO is an in-plane slipped π-type Al–Al antibonding/non-bonding orbital, and LUMO is an out-of-plane π-type Al–Al bonding orbital (Figure 4). In comparison, the highest occupied orbitals of base-stabilized dialuminenes, such as $Me^tBu_2Si(^{2iPr,2Me}NHC)AlAl(^{2iPr,2Me}NHC)SiMe^tBu_2$ (^{2iPr,2Me}NHC = 1,3-diisopropyl-4,5-dimethylimidazol-2-ylidene) by Inoue,[18] are σ- and π-type Al–Al bonding orbitals owing to the fulfilment of octet at each aluminum center. This difference can be rationalized by considering the electronic structures of $:AlAr^{iPr8}$ and $:Al(^{2iPr,2Me}NHC)SiMe^tBu_2$ in the context of the Carter-Goddard-Malrieu-Trinquier (CGMT) model.[19,20] The coordination by an external base results in significantly smaller singlet-triplet gap ($E_{T1}-E_{S0}$) for $:Al(^{2iPr,2Me}NHC)SiMe^tBu_2$ (ΔE_{ST} = 26 kJ mol^{-1}) than for $:AlAr^{iPr8}$ (ΔE_{ST} = 169 kJ mol^{-1}), which rationalizes the formation of a conventional Al=Al double bond in base-stabilized dialuminenes and a formally double dative bond in **1** and systems related to it.

Calculations probing the strength of bonding in **1** gave a standard bond dissociation ($Ar^{iPr8}AlAlAr^{iPr8} \rightarrow 2:AlAr^{iPr8}$) enthalpy and Gibbs free energy of 103 and 20 kJ mol^{-1}, respectively. A more detailed analysis of different bonding components using the energy decomposition analysis (EDA) revealed that electrostatic (−266 kJ mol^{-1}) and orbital (−222 kJ mol^{-1}) interactions outweigh Pauli repulsion (441 kJ mol^{-1}) only by a small margin. Consequently, dispersion interactions between two $:AlAr^{iPr8}$ fragments make a sizable contribution (−98 kJ mol^{-1}) to the calculated instantaneous interaction energy (−145 kJ mol^{-1}) and, therefore, are crucial for the stability of **1**. The calculated orbital interaction term can be expressed in terms of natural orbitals of chemical valence (NOCV), which revealed two

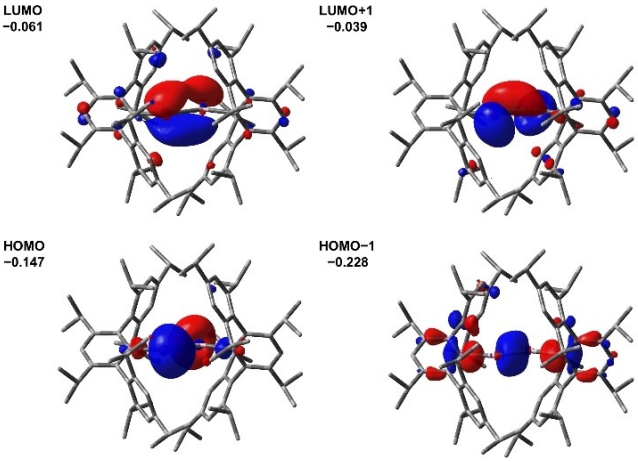

Figure 4. Isosurface (±0.04) plots of frontier Kohn-Sham orbitals of $Ar^{iPr8}AlAlAr^{iPr8}$ (**1**) with orbital energies given in atomic units. For clarity, hydrogen atoms are not shown.

major contributors. A visualization of the associated deformation densities indicated charge flow from the aluminum lone pairs to the Al–Al σ-bond as well as to the π-type slipped lone pairs formed upon bonding (see SI), in agreement with the description of the metal-metal bond as a weak double dative interaction.

Interestingly, the Kohn–Sham closed-shell singlet determinant of **1** shows a minor RHF to UHF instability, which indicates singlet diradical character in the wave function. This is reminiscent of the results obtained earlier for smaller model systems of **1**,[21] though in that case the diradical character manifested itself only in the Hartree-Fock determinant. The reoptimized broken-symmetry solution (UPBE1PBE-D3BJ/def2-TZVP) of **1** shows localization of opposite spin density around the aluminum atoms (see SI) and is only marginally lower in energy than the closed-shell singlet state. In the DFT formalism of electronic structure theory, static electron correlation effects, such as singlet diradical character, are primarily modeled by the exchange-correlation functional,[22] which explains why the observed instability is so small and a reasonably accurate description of the electronic structure is obtained even when using a spin-restricted ansatz. It is therefore expected that diradical character plays only a very small role in describing the reactivity of **1** which can be understood from a closed-shell perspective.[23] The frontier orbitals of **1** (Figure 4) are perfectly poised for both Lewis acid and base reactivity, rationalizing the extreme reactivity of free dialuminenes.[13] Consequently, the detailed characterization of **1** in solution along with all attempts to directly examine its reactivity proved unsuccessful. For this reason, the possible co-existence of :AlAr^{iPr8} and **1** in solution was examined indirectly by reacting :AlAr^{iPr8} with dihydrogen and ethylene, and comparing the observed reactivity with that known for other group 13 dimetallenes and metallenediyls.

Mechanism of the Reaction of :AlAr^{iPr8} with H_2

Recently, we reported that the alanediyl :AlAr^{iPr8} reacts rapidly with dihydrogen in C_6D_6, giving the dialane Ar^{iPr8}Al(H)(μ-H)$_2$Al(H)Ar^{iPr8} in high yield.[14] The facile formation of Ar^{iPr8}Al(H)(μ-H)$_2$Al(H)Ar^{iPr8} was surprising, considering that no similar reactivity has been reported for the gallium congener :GaAr^{iPr8} using the same terphenyl ligand.[24] In contrast, the digallene Ar^{iPr4}GaGaAr^{iPr4} is known to react with H_2 to afford the corresponding digallane Ar^{iPr4}Ga(H)(μ-H)$_2$Ga(H)Ar^{iPr4},[25] which implicates the metal-metal bonded dimer Ar^{iPr4}GaGaAr^{iPr4} as the reactive species in solution.[24] Consequently, we proposed that the facile reactivity of :AlAr^{iPr8} with H_2 can be explained with its in situ dimerization to Ar^{iPr8}AlAlAr^{iPr8} in solution.[14] Cowley and Krämer have recently reported a related base-coordinated dialuminene that can react either as the dimer or as the monomeric aluminyl in solution.[26] Further support for this proposal comes from reactivity described by Tokitoh for the benzene cycloadduct of (Bbp)AlAl(Bbp) (Bbp = C_6H_3-2,6-[CH(SiMe$_3$)$_2$]$_2$).[27] The cycloadduct readily dissociates in solution, allowing it to act as a synthetic equivalent of a dialuminene in subsequent reactions.[27–29]

The X-ray crystal structure of **1** (Figure 3) lends further, albeit indirect, support for the involvement of the dialuminene in the reaction of :AlAr^{iPr8} with H_2. To further test this hypothesis, the transition states for the addition of one and two equivalents of H_2 to :AlAr^{iPr8} and **1**, respectively, were modelled computationally in the gas phase. The results show that the direct addition of H_2 to :AlAr^{iPr8} is unlikely at room temperature, because the formation of Ar^{iPr8}AlH$_2$ is associated with a very high activation barrier (**TS-1**; $\Delta G^{\ddagger}$ = 192 kJ mol^{-1}) even though the reaction is mildly exergonic (ΔG = −67 kJ mol^{-1}). In contrast, the potential energy surface for the reaction of H_2 with **1** (Figure 5) shows a facile addition of the first equivalent of H_2 (**TS-2**; $\Delta G^{\ddagger}$ = 73 kJ mol^{-1}) along with a slightly higher barrier for the second addition (**TS-3**; $\Delta G^{\ddagger}$ = 101 kJ mol^{-1}). With this in mind, we investigated if an alternative pathway linking **1** and the dialane Ar^{iPr8}Al(H)(μ-H)$_2$Al(H)Ar^{iPr8} exists. The isomerization of the 1,2-dihydride intermediate Ar^{iPr8}Al(H)Al(H)Ar^{iPr8} is associated with a small barrier (**TS-4**; $\Delta G^{\ddagger}$ = 28 kJ mol^{-1}) and gives the 1,1-isomer Ar^{iPr8}Al(H)$_2$AlAr^{iPr8} (ΔG = 19 kJ mol^{-1}). This intermediate could dissociate to Ar^{iPr8}AlH$_2$ and :AlAr^{iPr8}, because the slightly endergonic (ΔG = 28 kJ mol^{-1}) breakup of the Al–Al bond is offset by the subsequent exergonic dimerization of Ar^{iPr8}AlH$_2$ (ΔG = −60 kJ mol^{-1}) and :AlAr^{iPr8} (ΔG = −20 kJ mol^{-1}), which offers another low-energy route to the dialane Ar^{iPr8}Al(H)(μ-H)$_2$Al(H)Ar^{iPr8}. Consequently, two pathways, both proceeding via the 1,2-dihydride intermediate Ar^{iPr8}Al(H)Al(H)Ar^{iPr8}, lead to Ar^{iPr8}Al(H)(μ-H)$_2$Al(H)Ar^{iPr8} whose formation from **1** and two equivalents of H_2 is overall highly exergonic (ΔG = −174 kJ mol^{-1}).

The computational results strongly support the notion that dimerization of alanediyls and gallanediyls to the corresponding dimetallenes is a prerequisite for observing reactivity with H_2 under ambient conditions. The reluctance of :GaAr^{iPr8} to react with H_2 can be explained, at least in

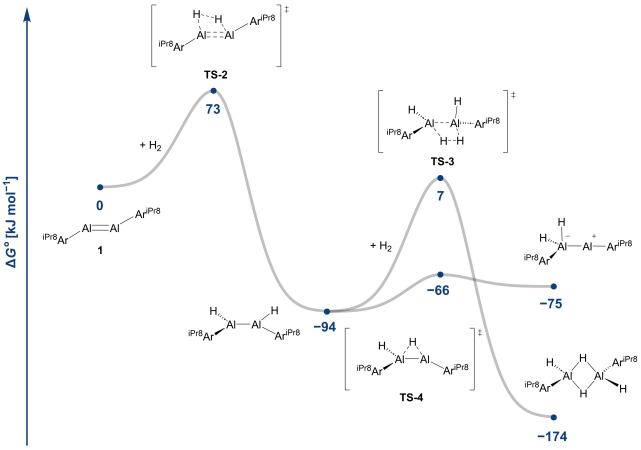

Figure 5. Calculated mechanism for the reaction of two equivalents of H_2 with Ar^{iPr8}AlAlAr^{iPr8}. Relative Gibbs energies refer to gas phase calculations at room temperature. For clarity, the dissociation of Ar^{iPr8}Al(H)$_2$AlAr^{iPr8} is not shown.

part, by the higher energies calculated for the key steps on the reaction paths shown in Figure 5. Specifically, the formation of the first intermediate has a considerably higher activation barrier for gallium ($\Delta G^{\ddagger} = 101\ kJ\,mol^{-1}$), which implies that the formation of the 1,2-dihydride $Ar^{iPr8}Ga(H)Ga(H)Ar^{iPr8}$ is slow at room temperature. As this intermediate is crucial for all subsequent routes leading to $Ar^{iPr8}Ga(H)(\mu\text{-}H)_2Ga(H)Ar^{iPr8}$, the digallane is not generated in any significant quantity under mild conditions. Another factor that plays a role in explaining the different reactivity between $:AlAr^{iPr8}$ and $:GaAr^{iPr8}$ is the change in metal-metal bonding from covalent to dispersive when going down the group.[21] Consequently, even though $Ar^{iPr8}AlAlAr^{iPr8}$ and $Ar^{iPr8}GaGaAr^{iPr8}$ are calculated to be equally stable in the gas phase ($\Delta G = -20\ kJ\,mol^{-1}$ and $-17\ kJ\,mol^{-1}$, respectively), a hydrocarbon solvent environment should exert a slightly stronger destabilizing effect on the latter, decreasing the likelihood of association of gallanediyls $:GaAr^{iPr8}$ and the probability of observing reactivity dependent on the dimetallene structure. This is in agreement with electronic spectroscopy and cryoscopy that have not shown any evidence for the association of $:GaAr^{iPr8}$ to $Ar^{iPr8}GaGaAr^{iPr8}$ in solution.[8,24]

Reaction of :AlAr^{iPr8} with C_2H_4

As a further attempt to investigate the interplay between the alanediyl $:AlAr^{iPr8}$ and **1** in solution, $:AlAr^{iPr8}$ was reacted with ethylene in C_6D_6 at room temperature. This led to two products that were identified by ^1H NMR spectroscopy. The minor product showed a singlet resonance at -0.80 ppm, suggesting the formation of $Ar^{iPr8}Al(C_2H_4)_2AlAr^{iPr8}$ (**2**, Figure 2) by analogy with the related digallenes.[30] The major product showed two broad resonances at ca. 1.49 and -0.56 ppm, each corresponding to four protons that are coupled to each other as shown by ^1H–^1H COSY NMR. The minor product could be isolated from the mixture at ca. 15 % yield and its identity confirmed by X-ray crystallography (Figure 6). However, despite repeated attempts, the major product could not be crystallized owing to its high solubility in hydrocarbon solvents. The ^1H NMR data allowed its tentative assignment as the aluminacyclopentane $Ar^{iPr8}Al(C_4H_8)$ (**3**, Figure 2) that most likely forms through coupling of two molecules of C_2H_4 by $:AlAr^{iPr8}$. In the absence of crystal data, the synthesis of **3** was attempted from $Ar^{iPr8}AlI_2$ and 1,4-$Li_2C_4H_8$, the latter of which has been used to prepare a related gallacyclopentane from $^tBu_2AsGaCl_2$.[31] The resulting white solid gave a ^1H NMR spectrum identical to that obtained for the major product from the reaction between $:AlAr^{iPr8}$ and C_2H_4, thereby confirming its identity as **3**.

The formation of **2** is reminiscent of the reactivity reported for the digallene $Ar^{iPr4}GaGaAr^{iPr4}$,[30] in which case a similar 1,4-digallacyclohexane core resulted from the addition of two equivalents of a terminal olefin across the Ga–Ga bond.[24] In contrast, the use of internal olefins or a bulky gallanediyl $:GaAr^{iPr8}$ lead to no reactivity with C_2H_4 at room temperature.[24,30] This result is in stark contrast to the

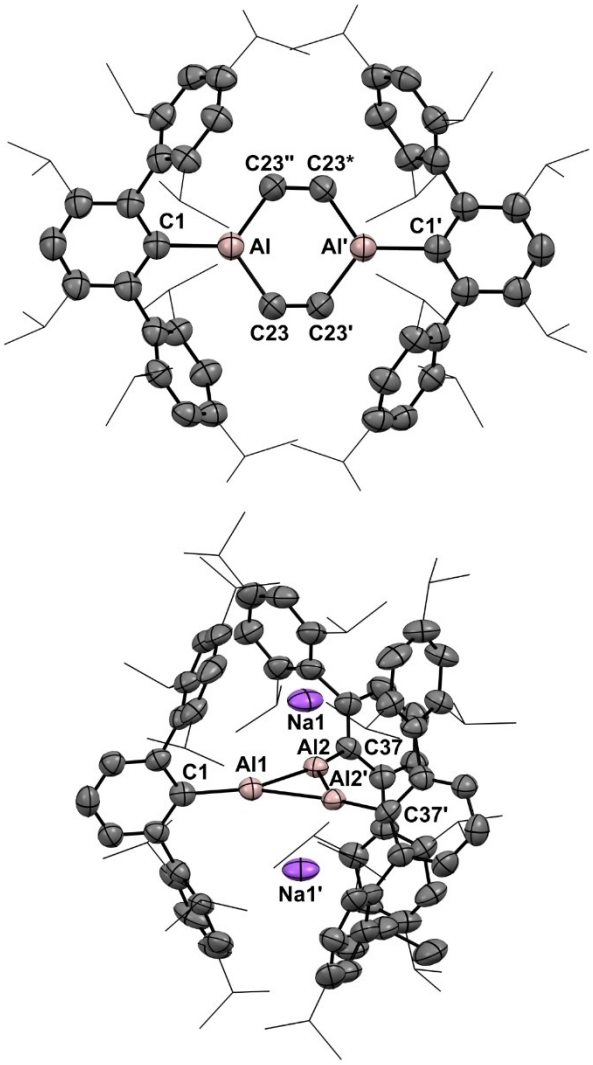

Figure 6. Single crystal X-ray structures of $Ar^{iPr8}Al(C_2H_4)_2AlAr^{iPr8}$ (**2**, top) and $Na_2[AlAr^{iPr6}]_3$ (**4**, bottom) with carbon atoms of the isopropyl groups shown in wireframe format and hydrogen atoms not shown. Thermal ellipsoids are drawn at 50 % probability level.

formation of **3** described herein. To shed more light on the mechanisms leading to **2** and **3** and the associated energy changes, the reactions of $:AlAr^{iPr8}$ and **1** with C_2H_4 were examined computationally in the gas phase.

The calculations revealed that the [2+2+2] cycloaddition of C_2H_4 to **1** is highly exergonic ($\Delta G = -288\ kJ\,mol^{-1}$). Interestingly, the transition state for the first addition (**TS-5**; $\Delta G^{\ddagger} = -6\ kJ\,mol^{-1}$) is slightly lower in energy than the combined Gibbs energies of isolated $Ar^{iPr8}AlAlAr^{iPr8}$ and C_2H_4, while the second addition of C_2H_4 to the 1,2-dialuminacyclobutane intermediate $Ar^{iPr8}Al(C_2H_4)AlAr^{iPr8}$ gives **2** without an identifiable activation barrier. In contrast, a well-defined transition state (**TS-6**; $\Delta G^{\ddagger} = 72\ kJ\,mol^{-1}$) was located for the addition of C_2H_4 to $:AlAr^{iPr8}$ (Figure 7), giving the aluminacylcopropane intermediate $Ar^{iPr8}Al(C_2H_4)$ in a slightly exergonic reaction ($\Delta G = -12\ kJ\,mol^{-1}$). The addition of a second equivalent of C_2H_4 to $Ar^{iPr8}Al(C_2H_4)$ was calculated to be barrierless and essentially energy

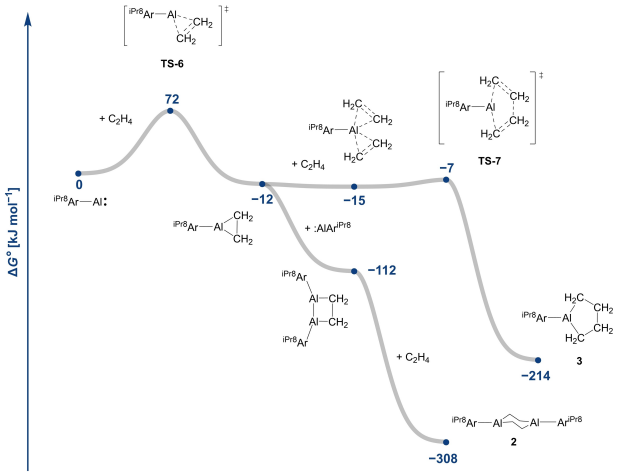

Figure 7. Calculated mechanism for the reaction of two equivalents of C_2H_4 with :$AlAr^{iPr8}$. Relative Gibbs energies refer to gas phase calculations at room temperature.

neutral, while the formation of the experimentally observed aluminacyclopentane **3** from $Ar^{iPr8}Al(C_2H_4)_2$ is highly exergonic ($\Delta G = -199\ kJ\,mol^{-1}$) and associated with a very small activation energy (**TS-7**; $\Delta G^{\ddagger} = 8\ kJ\,mol^{-1}$). We note that the aluminacylcopropane intermediate $Ar^{iPr8}Al(C_2H_4)$ can also react with another molecule of alanediyl :$AlAr^{iPr8}$ (Figure 7), giving the 1,2-dialuminacyclobutane intermediate in a single barrierless and exergonic step ($\Delta G = -100\ kJ\,mol^{-1}$). Subsequent reactivity of this intermediate with C_2H_4 provides another pathway to **2**.

The calculated mechanisms and energies agree with experimental observations, including the product distribution between **2** and **3**. The addition of two equivalents of C_2H_4 to **1** can give **2** via [2+2+2] cycloaddition. While this reaction is straightforward in silico, it is most likely hindered by steric factors associated with the array of isopropyl substituents surrounding the Al–Al bond. Consequently, even though the reaction between **1** and C_2H_4 is thermodynamically favorable, the steric environment most likely suppresses such reactivity at room temperature (cf. reactions of $Ar^{iPr4}GaGaAr^{iPr4}$ with internal olefins).[30] In a similar fashion, while the formation of **2** from the aluminacylcopropane intermediate (via 1,2-dialuminacyclobutane $(Ar^{iPr8}AlCH_2)_2$) is calculated to be exergonic, this pathway is sterically more hindered compared to the competitive reactivity of the same intermediate with C_2H_4 (Figure 7). As a result, **2** is a minor product from the reaction of :$AlAr^{iPr8}$ with C_2H_4. For these reasons, the pathway leading to **3** (Figure 7) is overall the most probable reaction route and it also gives a product that is thermodynamically the most favored when comparing the energy gain per equivalents of :$AlAr^{iPr8}$ used.

The above results indicate that the digallene $Ar^{iPr8}GaGaAr^{iPr8}$ should, in principle, undergo cycloaddition with C_2H_4, but the similarity of its steric environment to that in **1** speaks against such reactivity. Furthermore, there are no experimental data for the association of :$GaAr^{iPr8}$ in solution. The reluctance of :$GaAr^{iPr8}$ to react with C_2H_4 can, in turn, be rationalized by frontier orbital arguments as well as calculated energies. Specifically, the formation of the gallacylcopropane intermediate $Ar^{iPr8}Ga(C_2H_4)$ was found to be associated with a greater barrier compared to its aluminum congener ($\Delta G^{\ddagger} = 100$ vs. $72\ kJ\,mol^{-1}$), which implies that its formation is very slow at room temperature. Furthermore, the HOMO of gallacyclopropane is much higher in energy than the HOMO of gallanediyl or ethylene,[24] which explains why the formation of gallacyclopropane $Ar^{iPr8}Ga(C_2H_4)$ is moderately endergonic ($\Delta G = 53\ mol^{-1}$), while that of analogous aluminacyclopropane was calculated to be exergonic.

Attempted Synthesis of $Ar^{iPr6}AlAlAr^{iPr6}$

The one-coordinate geometry of the aluminum atom in the alanediyl :$AlAr^{iPr8}$ is enforced by the very large steric demand of the terphenyl ligand. Of key importance are the two isopropyl groups in the *meta*-positions of the central aryl ring as they influence the steric properties of the ligand by pushing the flanking aryl rings forward and limiting their rotation.[32,33] It was hypothesized that the removal of these groups, that is, using the known Ar^{iPr6} ligand, could allow stronger covalent association of alanediyls to the corresponding dialuminene, while at the same time providing sufficient steric protection to prevent any unwanted reactivity at the Al–Al bond.

The reduction of the etherate $Ar^{iPr6}AlI_2(OEt_2)$ with an excess of Na on NaCl in hexanes gave a dark red solution within 24 h. Filtration and concentration of the solution, followed by storage at ca. 5 °C, resulted in dark red crystals that were suitable for X-ray crystallography. Interestingly, the reduction had yielded the sodium salt of the cyclotrialuminene, $Na_2[AlAr^{iPr6}]_3$ (**4**, Figure 2). The structure of **4** (Figure 6) is centrosymmetric with a triangular Al_3 ring (avg. Al–Al distance of 2.556 Å) oriented almost perpendicularly (85.4°) to one of the central aryl rings of the Ar^{iPr6} ligands, while the two other central rings form an almost half right angle (49.0°) with the Al_3 plane. The two disordered sodium cations are located symmetrically above and below the centroid of the Al_3 core (avg. Na···Al_3 distance of 2.841 Å) and coordinated to the flanking aryl rings of the Ar^{iPr6} ligands. The structure of **4** resembles closely those of $Na_2[AlAr^{Me6}]_3$[2] and $Na_2[GaAr^{Me6}]_3$[34] that both employ a terphenyl ligand with the same substitution pattern but lower steric bulk. An analysis of metalloaromaticity in these two π-electron systems has been presented.[35] Apparently, the Al–Al interactions in **4** are sufficiently strong to render the trimeric structure energetically preferred over the dimer $Na_2[AlAr^{iPr6}]_2$. For comparison, the reduction of $Ar^{iPr6}GaCl_2$ with excess Na is known to give the digallyne $Na_2[GaAr^{iPr6}]_2$,[1] with no evidence of the formation of the trimer $Na_2[GaAr^{iPr6}]_3$. All attempts to reduce the etherate $Ar^{iPr6}AlI_2(OEt_2)$ with a stoichiometric amount of Na on NaCl in hexanes resulted in intractable mixtures.

Recently, the comproportionation reaction between the dialuminyne $Na_2[Al(Ar^{iPr4}\text{-}4\text{-}SiMe_3)]_2$ and its precursor iodides $(Ar^{iPr4}\text{-}4\text{-}SiMe_3)AlI_2(OEt_2)$ or $(Ar^{iPr4}\text{-}4\text{-}SiMe_3)(I)AlAl$

(I)(Ar^{iPr4}-4-$SiMe_3$) was reported to result in the highly reactive dialuminene (Ar^{iPr4}-4-$SiMe_3$)AlAl(Ar^{iPr4}-4-$SiMe_3$) in situ.[13] Following this approach, the reaction between **4** and the etherate $Ar^{iPr6}AlI_2(OEt_2)$ was attempted with the intention of generating a new neutral aluminum species, possibly $Ar^{iPr6}AlAlAr^{iPr6}$. However, mixing the two compounds in C_6D_6 did not result in any observable reaction even upon prolonged heating. It is likely that the three large Ar^{iPr6} ligands in **4** shield its central Al_3 ring sufficiently, preventing the desired redox reaction from taking place.

Conclusion

Through meticulous analysis of single crystal X-ray diffraction data, we have shown that the green crystals formed in the non-stoichiometric reduction of $Ar^{iPr8}AlI_2$ with Na on NaCl are those of the sought-after solvent-free dialuminene $Ar^{iPr8}AlAlAr^{iPr8}$ (**1**) which forms alongside the yellow-orange crystals of the alanediyl :$AlAr^{iPr8}$. The X-ray crystal structure of **1** shows the expected planar, *trans*-bent C(ipso)AlAlC(ipso) core with an Al–Al distance of 2.648(2) Å. DFT calculations reproduce the key structural features of **1** and describe its Al–Al bond as a weak donor-acceptor interaction augmented with diradical character and stabilized by dispersion interactions. The dialuminene **1** shows extreme reactivity, with re-solvation of the crystals leading to dissociation to alanediyl monomers and formation of Al–H moieties, as shown by spectroscopy.

DFT calculations on the mechanism of the reaction of the alanediyl :$AlAr^{iPr8}$ with dihydrogen identify the dialuminene **1** as the key species. Two competitive pathways are found, both of which lead to the experimentally characterized dialane $Ar^{iPr8}Al(H)(\mu\text{-}H)_2Al(H)Ar^{iPr8}$. In contrast, the direct addition of H_2 to :$AlAr^{iPr8}$ is associated with a very high energy barrier, making this route improbable under ambient conditions. Based on the results from single crystal X-ray crystallography and ^1H NMR spectroscopy, the reaction of :$AlAr^{iPr8}$ with ethylene yields 1,4-dialuminacyclohexane $Ar^{iPr8}Al(C_2H_4)_2AlAr^{iPr8}$ (**2**) as the minor product and aluminacyclopentane $Ar^{iPr8}Al(C_4H_8)$ (**3**) as the major product. Mechanistic modelling by DFT shows that both products can form from the aluminacylcopropane intermediate $Ar^{iPr8}Al(C_2H_4)$ upon successive reactions with :$AlAr^{iPr8}$ and C_2H_4 (**2**) or C_2H_4 (**3**). Even though the [2+2+2] cycloaddition between **1** and two equivalents of C_2H_4 is calculated to be exergonic, it is most likely hindered by the protective sphere of isopropyl substituents surrounding the Al–Al bond. Results from DFT calculations also rationalize the difference in reactivity of :$GaAr^{iPr8}$ with H_2 and C_2H_4 in comparison to its lighter aluminum congener.

Attempts to synthesize a less bulky, yet solvent-free dialuminene $Ar^{iPr6}AlAlAr^{iPr6}$ through reduction and comproportionation routes were unsuccessful, leading to the isolation and characterization of the sodium salt of the cyclotrialuminene $Na_2[AlAr^{iPr6}]_3$ (**4**). While suitable electronic and structural modifications to the terphenyl ligand may yield further examples of isolable dialuminenes in the future, their inherent reactivity and instability is a consequence of their ability to react both as a Lewis acid and a base, with diradical character playing only a minor role. This allows a wide variety of transformations to take place, possibly even ones involving the most inert of chemical species. Mechanistic investigations of reactions involving solvent stabilized dialuminenes with a wide variety of small molecules are currently underway.

Supporting Information

Experimental and characterization details for all new compounds, including spectroscopic and crystallographic data,[36] as well as optimized structures (*xyz*-coordinates). The authors have cited additional references within the Supporting Information.[37–61]

Acknowledgements

We thank the National Science Foundation (CHE-2152760 and CHE-1531193) for supporting this work. This project received funding from the European Research Council under the European Union's Horizon 2020 research and innovation programme (Grant No. 772510 to H.M.T.). We thank Dr. James C. Fettinger for collecting the X-ray data.

Conflict of Interest

The authors declare no conflict of interest.

Data Availability Statement

The data that support the findings of this study are available in the supplementary material of this article.

Keywords: main group elements · aluminum · multiple bonds · reaction mechanisms · density functional calculations

[1] J. Su, X.-W. Li, C. Crittendon, G. H. Robinson, *J. Am. Chem. Soc.* **1997**, *119*, 5471–5472. https://doi.org/10.1021/ja9700562.
[2] R. J. Wright, M. Brynda, P. P. Power, *Angew. Chem. Int. Ed.* **2006**, *45*, 5953–5956. https://doi.org/10.1002/anie.200601925.
[3] N. J. Hardman, R. J. Wright, A. D. Phillips, P. P. Power, *Angew. Chem. Int. Ed.* **2002**, *41*, 2842–2844. https://doi.org/10.1002/1521-3773(20020802)41:15<2842::AID-ANIE2842>3.0.CO;2-O.
[4] R. J. Wright, A. D. Phillips, N. J. Hardman, N. P. P. Power, *J. Am. Chem. Soc.* **2002**, *124*, 8538–8539. https://doi.org/10.1021/ja026285s.
[5] R. J. Wright, A. D. Phillips, S. Hino, P. P. Power, *J. Am. Chem. Soc.* **2005**, *127*, 4749–4799. https://doi.org/10.1021/ja0432259.
[6] S. T. Haubrich, P. P. Power, *J. Am. Chem. Soc.* **1998**, *120*, 2202–2203. https://doi.org/10.1021/ja973479c.
[7] M. Niemeyer, P. P. Power, *Angew. Chem. Int. Ed.* **1998**, *37*, 1277–1279. https://doi.org/10.1002/(SICI)1521-3773(19980518)37:9<1277::AID-ANIE1277>3.3.CO;2-T.

[8] Z. Zhu, R. C. Fischer, B. D. Ellis, E. Rivard, W. A. Merrill, M. M. Olmstead, P. P. Power, J. D. Guo, S. Nagase, L. Pu, *Chem. Eur. J.* **2009**, *15*, 5263–5272. https://doi.org/10.1002/chem.200900201.
[9] F. A. Cotton, A. H. Cowley, X. Feng, *J. Am. Chem. Soc.* **1998**, *120*, 1795–1799. https://pubs.acs.org/doi/10.1021/ja973015e.
[10] I. Bytheway, Z. Lin, *J. Am. Chem. Soc.* **1998**, *120*, 12133–12134. https://doi.org/10.1021/ja981851y.
[11] T. L. Allen, H. F. William, P. P. Power, *J. Chem. Soc. Dalton Trans.* **2000**, 407–412. https://doi.org/10.1039/A907421 J.
[12] R. J. Wright, A. D. Phillips, P. P. Power, *J. Am. Chem. Soc.* **2003**, *125*, 10784–10785. https://doi.org/10.1021/ja034478p.
[13] J. D. Queen, P. P. Power, *Chem. Commun.* **2023**, *59*, 43–46. https://doi.org/10.1039/D2CC05646A.
[14] J. D. Queen, A. Lehmann, J. C. Fettinger, H. M. Tuononen, P. P. Power, *J. Am. Chem. Soc.* **2020**, *142*, 20554–20559. https://doi.org/10.1021/jacs.0c10222.
[15] J. C. Fettinger, P. A. Gray, C. E. Melton, P. P. Power, *Organometallics* **2014**, *33*, 6232–6240. https://doi.org/10.1021/om500911f.
[16] C. E. Melton, J. W. Dube, P. J. Ragogna, J. C. Fettinger, P. P. Power, *Organometallics* **2014**, *33*, 329–337. https://doi.org/10.1021/om4010675.
[17] D. Dhara, A. Jayaraman, M. Märterich, R. D. Dewhurst, H. Braunschweig, *Chem. Sci.* **2022**, *13*, 5631–5638. https://doi.org/10.1039/D2SC01436J.
[18] P. Bag, A. Porzelt, P. J. Altmann, S. Inoue, *J. Am. Chem. Soc.* **2017**, *139*, 14384–14387. https://doi.org/10.1021/jacs.7b08890.
[19] E. A. Carter, W. A. Goddard III, *J. Phys. Chem.* **1986**, *90*, 998–1001. https://doi.org/10.1021/j100278a006.
[20] G. Trinquier, J.-P. Malrieu, *J. Am. Chem. Soc.* **1987**, *109*, 5303–5315. https://doi.org/10.1021/ja00252a002.
[21] J. Moilanen, P. P. Power, H. M. Tuononen, *Inorg. Chem.* **2010**, *49*, 10992–11000. https://doi.org/10.1021/ic101487g.
[22] D. Cremer, *Mol. Phys.* **2001**, *99*, 1899–1940. https://doi.org/10.1080/00268970110083564.
[23] T. Stuyver, B. Chen, T. Zeng, P. Geerlings, F. De Proft, R. Hoffmann, *Chem. Rev.* **2019**, *119*, 11291–11351. https://doi.org/10.1021/acs.chemrev.9b00260.
[24] C. A. Caputo, J. Koivistoinen, J. Moilanen, J. N. Boynton, H. M. Tuononen, P. P. Power, *J. Am. Chem. Soc.* **2013**, *135*, 1952–1960. https://doi.org/10.1021/ja3116789.
[25] Z. Zhu, X. Wang, Y. Peng, H. Lei, J. C. Fettinger, E. Rivard, P. P. Power, *Angew. Chem. Int. Ed.* **2009**, *48*, 2031–2034. https://doi.org/10.1002/anie.200805982.
[26] R. L. Falconer, K. M. Byrne, G. S. Nichol, T. Krämer, M. J. Cowley, *Angew. Chem. Int. Ed.* **2021**, *60*, 24702–24708. https://doi.org/10.1002/anie.202111385.
[27] T. Agou, K. Nagata, N. Tokitoh, *Angew. Chem. Int. Ed.* **2013**, *52*, 10818–10821. https://doi.org/10.1002/anie.201305228.
[28] T. Agou, K. Nagata, T. Sasamori, N. Tokitoh, *Chem. Asian J.* **2014**, *9*, 3099–3101. https://doi.org/10.1002/asia.201402798.
[29] K. Nagata, T. Murosaki, T. Agou, T. Sasamori, T. Matsuo, N. Tokitoh, *Angew. Chem. Int. Ed.* **2016**, *55*, 12877–12880. https://doi.org/10.1002/anie.201606684.
[30] C. A. Caputo, Z. Zhu, Z. D. Brown, J. C. Fettinger, P. P. Power, *Chem. Commun.* **2011**, *47*, 7506–7508. https://doi.org/10.1039/C1CC11676B.
[31] A. H. Cowley, S. Corbelin, R. A. Jones, R. J. Lagow, J. W. Nail, *J. Organomet. Chem.* **1994**, *464*, C1–C3. https://doi.org/10.1016/0022-328X(94)87019–5.
[32] C. Stanciu, A. F. Richards, J. C. Fettinger, M. Brynda, P. P. Power, *J. Organomet. Chem.* **2006**, *691*, 2540–2545. https://doi.org/10.1016/j.jorganchem.2006.01.046.
[33] Z. Zhu, R. C. Fischer, B. D. Ellis, E. Rivard, A. Merrill, M. M. Olmstead, P. P. Power, J. D. Guo, S. Nagase, L. Pu, *Chem. Eur. J.* **009**, *15*, 5263–5272. https://doi.org/10.1002/chem.200900201.
[34] X.-W. Li, W. T. Pennington, G. H. Robinson, *J. Am. Chem. Soc.* **1995**, *117*, 7578–7579. https://doi.org/10.1021/ja00133a045.
[35] X.-W. Li, Y. Xie, P. R. Schreiner, K. D. Gripper, R. C. Crittendon, C. F. Campana, H. F. Schaefer, G. H. Robinson, *Organometallics* **1996**, *15*, 3798–3803. https://doi.org/10.1021/ja9616701.
[36] Deposition numbers CCDC 2353348 (**1**), 2353348 (**2**), 2353350 (**4**) and 2355052 (**5**) contain the supplementary crystallographic data for this paper. These data are provided free of charge by the joint Cambridge Crystallographic Data Centre and Fachinformationszentrum Karlsruhe Access Structures service.
[37] A. B. Pangborn, M. A. Giardello, R. H. Grubbs, R. K. Rosen, F. J. Timmers, *Organometallics* **1996**, *15*, 1518–1520. https://doi.org/10.1021/om9503712.
[38] G. R. Fulmer, A. J. M. Miller, N. H. Sherden, H. E. Gottlieb, A. Nudelman, B. M. Stoltz, J. E. Bercaw, K. I. Goldberg, *Organometallics* **2010**, *29*, 2176–2179. https://doi.org/10.1021/om100106e.
[39] R. J. Wehmschulte, W. J. Grigsby, B. Schiemenz, R. A. Bartlett, P. P. Power, *Inorg. Chem.* **1996**, *35*, 6694–6702. https://doi.org/10.1021/ic960486d.
[40] J. Hicks, M. Juckel, A. Paparo, D. Dange, C. Jones, *Organometallics* **2018**, *37*, 4810–4813. https://doi.org/10.1021/acs.organomet.8b00803.
[41] CrysAlis^{Pro}, version 1.173.42.49, Rigaku, **2022**.
[42] SAINT, Version 8.37a, Bruker AXS Inc., Madison, Wisconsin, USA, **2015**.
[43] Sheldrick, G. M. SADABS: Program for Empirical Absorption Correction of Area Detector Data, University of Göttingen, Göttingen, Germany, **1996**.
[44] G. M. Sheldrick, *Acta Crystallogr. Sect. A* **2015**, *71*, 3–8. https://doi.org/10.1107/S2053273314026370.
[45] O. V. Dolomanov, L. J. Bourhis, R. J. Gildea, J. A. K. Howard, H. Puschmann, *J. Appl. Crystallogr.* **2009**, *42*, 339–341. https://doi.org/10.1107/S0021889808042726.
[46] G. M. Sheldrick, *Acta Crystallogr. Sect. C* **2015**, *71*, 3–8. https://doi.org/10.1107/S2053229614024218.
[47] J. P. Perdew, K. Burke, M. Ernzerhof, *Phys. Rev. Lett.* **1996**, *77*, 3865–3868. https://doi.org/10.1103/PhysRevLett.77.3865.
[48] J. P. Perdew, K. Burke, M. Ernzerhof, *Phys. Rev. Lett.* **1996**, *78*, 1396. https://doi.org/10.1103/PhysRevLett.78.1396.
[49] C. Adamo, V. Barone, *J. Chem. Phys.* **1999**, *110*, 6158–6170. https://doi.org/10.1063/1.478522.
[50] M. Ernzerhof, G. E. Scuseria, *J. Chem. Phys.* **1999**, *110*, 5029–5036. https://doi.org/10.1063/1.478401.
[51] F. Weigend, R. Ahlrichs, *Phys. Chem. Chem. Phys.* **2005**, *7*, 3297–3305. https://doi.org/10.1039/B508541A.
[52] S. Grimme, J. Antony, S. Ehrlich, H. Krieg, *J. Chem. Phys.* **2010**, *132*, 154104. https://doi.org/10.1063/1.3382344.
[53] S. Grimme, S. Ehrlich, L. Goerigk, *J. Comput. Chem.* **2011**, *32*, 1456–1465. https://doi.org/10.1002/jcc.21759.
[54] Gaussian 16, Revision C.01, M. J. Frisch, G. W. Trucks, H. B. Schlegel, G. E. Scuseria, M. A. Robb, J. R. Cheeseman, G. Scalmani, V. Barone, G. A. Petersson, H. Nakatsuji, X. Li, M. Caricato, A. V. Marenich, J. Bloino, B. G. Janesko, R. Gomperts, B. Mennucci, H. P. Hratchian, J. V. Ortiz, A. F. Izmaylov, J. L. Sonnenberg, D. Williams-Young, F. Ding, F. Lipparini, F. Egidi, J. Goings, B. Peng, A. Petrone, T. Henderson, D. Ranasinghe, V. G. Zakrzewski, J. Gao, N. Rega, G. Zheng, W. Liang, M. Hada, M. Ehara, K. Toyota, R. Fukuda, J. Hasegawa, M. Ishida, T. Nakajima, Y. Honda, O. Kitao, H. Nakai, T. Vreven, K. Throssell, J. A. Montgomery, Jr., J. E. Peralta, F. Ogliaro, M. J. Bearpark, J. J. Heyd, E. N. Brothers, K. N. Kudin, V. N. Staroverov, T. A. Keith, R. Kobayashi, J. Normand, K. Raghavachari, A. P. Rendell, J. C.

Burant, S. S. Iyengar, J. Tomasi, M. Cossi, J. M. Millam, M. Klene, C. Adamo, R. Cammi, J. W. Ochterski, R. L. Martin, K. Morokuma, O. Farkas, J. B. Foresman, and D. J. Fox, Gaussian, Inc., Wallingford CT, **2016**.
[55] K. Morokuma, *J. Chem. Phys.* **1971**, *55*, 1236–1244. https://doi.org/10.1063/1.1676210.
[56] T. Ziegler, A. Rauk, *Theor. Chim. Acta* **1977**, *46*, 1–10. https://doi.org/10.1007/BF02401406.
[57] M. P. Mitoraj, A. Michalak, T. A. Ziegler, *J. Chem. Theory Comput.* **2009**, *5*, 962–975. https://doi.org/10.1021/ct800503d.
[58] ADF 2019.3, SCM, Theoretical Chemistry, Vrije Universiteit, Amsterdam, The Netherlands, **2019**.
[59] E. van Lenthe, E. J. Baerends, *J. Comput. Chem.* **2003**, *24*, 1142–1156. https://doi.org/10.1002/jcc.10255.
[60] E. van Lenthe, E. J. Baerends, J. G. Snijders, *J. Chem. Phys.* **1994**, *101*, 9783–9792. https://doi.org/10.1063/1.467943.
[61] E. Negishi, D. R. Swanson, C. J. Rousset, *J. Org. Chem.* **1990**, *55*, 5406–5409. https://dx.doi.org/10.1021/jo00306a022.

Manuscript received: July 4, 2024
Accepted manuscript online: August 19, 2024
Version of record online: October 24, 2024